IEEE Access
Multidisciplinary | Rapid Review | Open Access Journal

Received 10 September 2023, accepted 27 September 2023, date of publication 29 September 2023,
date of current version 4 October 2023.

Digital Object Identifier 10.1109/ACCESS.2023.3320806

RESEARCH ARTICLE

Study on High Energy Discharge Characteristics Caused by Arc Faults in Transformer Turret

SHIHONG HU[1,2], ZHICHENG HUANG[1,2], XI LIU[1,2], JIAHUI CHEN[1,2], YAN WANG[1,2], TAO ZHAO[3], (Member, IEEE), AND CHAOJIE YANG[3]

[1]State Grid Sichuan Electric Power Research Institute, Chengdu 610000, China
[2]Power Internet of Things Key Laboratory of Sichuan Province, Chengdu 610000, China
[3]Hebei Provincial Key Laboratory of Power Transmission Equipment Security Defense, North China Electric Power University, Baoding 071003, China

Corresponding author: Chaojie Yang (1140291840@qq.com)

This work was supported in part by the Science and Technology Project of State Grid Sichuan Electric Power Company under Grant 52199722000U.

ABSTRACT The power transformer is an essential equipment in the UHV transmission system. High energy discharge resulting from arc faults in the transformer turret can lead to an explosion, posing a serious threat to the safe and stable operation of the power system. At present, there is a lack of experimental research on arc discharge faults in the transformer turret. The ignition and explosion process remains unclear, which limits the improvement of transformer explosion-proof performance. To address this issue, a test platform of arc discharge fault in the transformer turret was constructed. High-current and high-deflagration capacity simulation short-circuit tests were carried out, and the voltage and current waveforms in the arc discharge process were obtained. This facilitated the quantitative characterization of discharge energy and analysis of the arc energy flow conversion. The test results highlighted that arc energy and arc current are the important factors affecting the voltage boost in the riser. The arc process of casing rupture under high current (1400 A) can be divided into two stages: ''smooth'' and ''sudden''. The insulating oil after high energy discharge and the gas escaping from the oil were analyzed by chromatographic methods. The results revealed that the oil cracking occurs after high energy discharge, significantly increasing various fault characteristic gases in the oil. Among these gases, H_2, CH_4, C_2H_2, and C_2H_4 exhibited the highest total content in the oil, while H_2, CH_4, and C_2H_4 presented the greatest range in the escaped gas, accounting for more than 75% of the total volume. This work elucidates the physical mechanism of the internal short-circuit fault of the transformer turret, and holds crucial guiding significance for the transformer explosion-proof design.

INDEX TERMS Transformer turret, arc failure, high energy discharge, arc energy, chromatographic analysis.

I. INTRODUCTION

The UHV transmission technology has been widely adopted due to its notable advantages, such as low transmission loss, high land utilization rate and long transmission distance. Compared with ordinary transformers, UHV transformers face unique challenges, including operating at high voltages, accommodating large oil volumes, necessitating stringent insulation require-ments, and experiencing an increased probability of insulation breakdown, which may result in a greater risk of accidents [1], [2], [3].

When there is a short-circuit fault inside the transformer riser, a substantial amount of energy is rapidly released by the arc. That causes the surrounding insulating oil to crack and gasify, resulting in gas expansion and a sudden increase in pressure inside the equipment [4], [5], [6]. Once the pressure surpasses the structural limits of the enclosure, cracks can occur, and even an explosion may transpire [7], posing severe risks to the safety of equipment, buildings, and personnel [8], [9].

To avoid transformer explosion accidents, since the 1950s, some scholars have paid extensive attention to transformer fuel tank cracking, explosion and even fire accidents caused by arc faults [10], [11], [12]. In recent decades, transformer

The associate editor coordinating the review of this manuscript and approving it for publication was Norbert Herencsar.

manufacturers and universities have modeled and analyzed the physical mechanism of high energy discharge caused by transformer internal arc faults. Additionally, experiments have been conducted to advance the understanding of this field further [13], [14], [15], [16], [17].

In 1960, scholar R. J. Ringlee used high-pressure nitrogen to simulate the arc fault in a transformer [18]. While relatively simple, safe and reproducible, this method does not generate gas as rapidly as a real arc. Between 2002 and 2004, 62 experiments on transformer internal faults were carried out in France and Brazil [13]. Although the primary objective of these experiments was to verify the performance of French SERGI's oil discharge and nitrogen injection equipment on transformer protection, they served as valuable reference cases for conducting arc fault tests by using real transformers. In 2020, Liu Zehong et al. conducted a 500kV actual arc fault pressure characteristic test at the Suzhou Electric Power Research Science Institute. During this test, the maximum arc energy recorded was 56 MJ, and the pressure data in the turret area were obtained [19].

When the arc fault occurs, the insulating oil near the arc path undergoes rapid gasification and cracking, and a large amount of gas is generated along with the physical and chemical reactions.

In 1953, scholar Henry Trencham first proposed that there is a direct proportional relationship between the gas generated by arc faults and the arc energy [4]. Scholar Tomo Tadokoro [5] from CRIEPI in Japan further observed that gas production is saturated when the arc fault energy reaches a certain level (MJ level). That occurs when most of the insulating oil around the arc channel is vaporized and cracked, forming a bubble that envelops the entire arc channel. At this point, the arc energy primarily serves to heat the gas and decompose the vaporized oil, forming secondary products. The energy is no longer available to further gasify and decompose additional insulation oil, leading to a decrease in the rate of gas production as the arc persists. There exists a logarithmic relationship between gas production and arc energy. It is generally believed that the relationship between gas production and arc energy in oil at normal temperature and pressure is about 50-100 mL/kJ.

Due to the substantial risk and significant cost associated with large-scale on-site power transformer arc failure tests, researchers generally abstain from conducting actual type tests. Consequently, there is a lack of experimental studies on arc current and deflagration energy comparable to the actual transformer arc discharge faults. As a result, the existing studies fail to capture the genuine high-energy discharge characteristics of large-capacity transformer arc faults.

In this research endeavor, a specialized test platform was constructed to investigate high-energy discharges caused by arc faults in the transformer turret area, and the actual type simulation tests of arc discharge faults at currents of 800 A and 1400 A were carried out. The novelty lies in the fact that the quantitative characterization of turret model high-energy discharge current, voltage and discharge energy is obtained by obtaining the specific relationship of voltage, current and energy during the arc discharge process through the independently constructed high-energy discharge test system. And auxiliary oil chromatography analysis of insulating oil cracking gasification characteristics, obtained the high energy discharge case insulation degradation led to material cracking, gasification development speed characteristics and gas component characterization of the change rule. This endeavor has achieved initial success in unraveling the physical mechanism underlying the internal short-circuit fault of the transformer riser, providing vital insights for the design of explosion-proof measures in transformers.

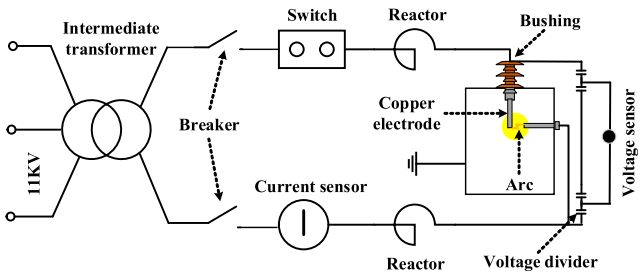

FIGURE 1. The system loop for arcing fault tests.

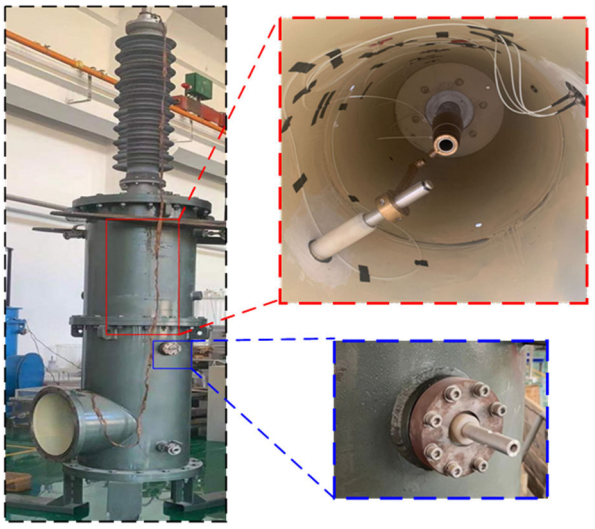

FIGURE 2. Arc triggering device and sensor arrangement diagram.

II. EXPERIMENT

A. EXPERIMENTAL LOOP

In the arc fault experiment, it is imperative to have an experimental power supply capable of delivering a kiloamp arc current.

As shown in Fig. 1, the circuit of the experimental system primarily comprises an intermediate transformer, switch, circuit breaker, reactor, current sensor, voltage sensor, voltage divider and lifting seat. The voltage signal is collected by the voltage divider and voltage sensor, and the current signal

is collected by the Roche coil as the current sensor. The intermediate transformer is connected to an 11 kV AC grid.

B. EXPERIMENTAL PLATFORM

The height of the elevated seat for the test turret is 4285 mm, the diameter of the base is 1600 mm, and the total weight of the empty test chamber is about 800 kg. The physical layout and components of the arc fault test platform are shown in Fig. 2. The cavity is designed in a cylindrical structure. During the test, the arc current is introduced through the top sleeve and guided via the flange in the middle side wall, as shown in the blue box in Fig. 2. The electrode spacing of the copper row is set at 30 mm, and the copper wire with a diameter of 0.5 mm is used as the arc-initiating wire, as shown in the red box in Fig. 2. The high energy discharge test meets the relevant IEC and IEEE standards [20], [21], [22], [23], [24].

C. AIR COLLECTION DEVICE

The air collection device comprises five parts: N_2 high-pressure gas cylinder, vacuum pump, vacuum air collecting bag, air valve, and explosive-proof hose, as shown in Figure 3. Specifically, the air valves labeled as V_1-V_4 are 1/4 NPT internal and external thread stainless steel ball valves; the valve used for V5 is a bamboo ball valve, with one end featuring a 1/4 NPT external thread and the other equipped with a bamboo joint of 8mm outer diameter, which is convenient for connecting with the hose between the assembly bag. The valve core exhibits a pressure tolerance of ±2.5 MPa. The explosion-proof hose is made of stainless steel high-pressure bellows with a 6mm inner diameter. It can withstand pressures within the range of 0-20 MPa, and exhibits a maximum temperature tolerance of 200 °C. Both ends of the hose are equipped with 1/4 NPT internal threads.

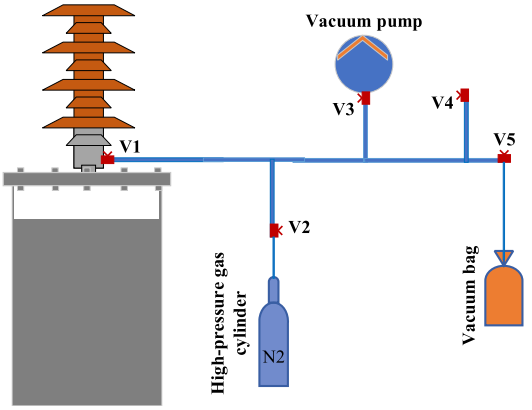

FIGURE 3. Gas collection device test platform.

The crucial parts between the flange and the cavity are sealed by fluorine rubber.

The insulating oil underwent dissolved gas chromatography analysis before and after the test. At the same time, the gas was collected through the vent valve and subsequently analyzed. After the arc wire was melted and ruptured, the cavity was opened to replace the arc wire. In this process, the transformer oil was subjected to filtration using an oil filter to remove impurities, and after treatment, the oil was re-injected for subsequent testing.

D. VALVE SWITCH STATUS AND WORKING MODE

A closed path containing multiple valves was designed and built to meet the requirements of sample handling, pressure regulation, sampling and other operations during the test, and minimize the interference of external factors on the test results. The primary operations in the test include cavity pressure test, cavity inlet and washing, vacuum extraction and gas sampling. In order to realize the above functions, the valves were adjusted accordingly to switch the connection mode between the test chamber and the surrounding supporting devices. Table 1 shows the switching status of each valve in different working modes.

TABLE 1. The switching state of each valve under different working modes. a value of 1 indicates an open state, while a value of 0 indicates a closed state.

	Mode	V_1	V_2	V_3	V_4	V_5	Operation
Before test	I	1	1	0	0	0	Chamber pressure test
	II	1	0	1	0	0	Vacuum extraction
In test	III	0	0	0	0	0	In test
After test	IV	1	0	0	1	0	Residual gas evacuation
	V	1	0	0	0	1	Gas collection

III. RESULTS

A. RESULTS OF HIGH ENERGY DISCHARGE

In general, the short-circuit arc fault current in the elevated seat of the transformer is generally 500-40000 A [20]. The purpose of this work is to find the weak position of the transformer turret, and to improve the weak point, so the experiment is not set up the pressure relief valve. The experimental current follows the principle of increasing from low to high, so the discharge current level is selected at 800 A and 1400 A.

For 50-60 Hz currents, the typical duration is 2 to 3 cycles. The arc time determines the size of the arc discharge energy. Therefore, in order to observe a complete arc-firing process, this paper will each test current arc-firing time control within 500 ms, such as 500 ms arc extinguished within the stop, such as continued after 500 ms cut off the power supply.

1) 800 A

Arc voltage, current and energy measured in the 800 A arc fault test are shown in Fig. 4.

As shown in Fig. 4, the arc burning time of this test was 420 ms. The practical value of arc current was approximately 800 A, exhibiting a sine-wave waveform with some DC components. At the beginning of the arc, the voltage

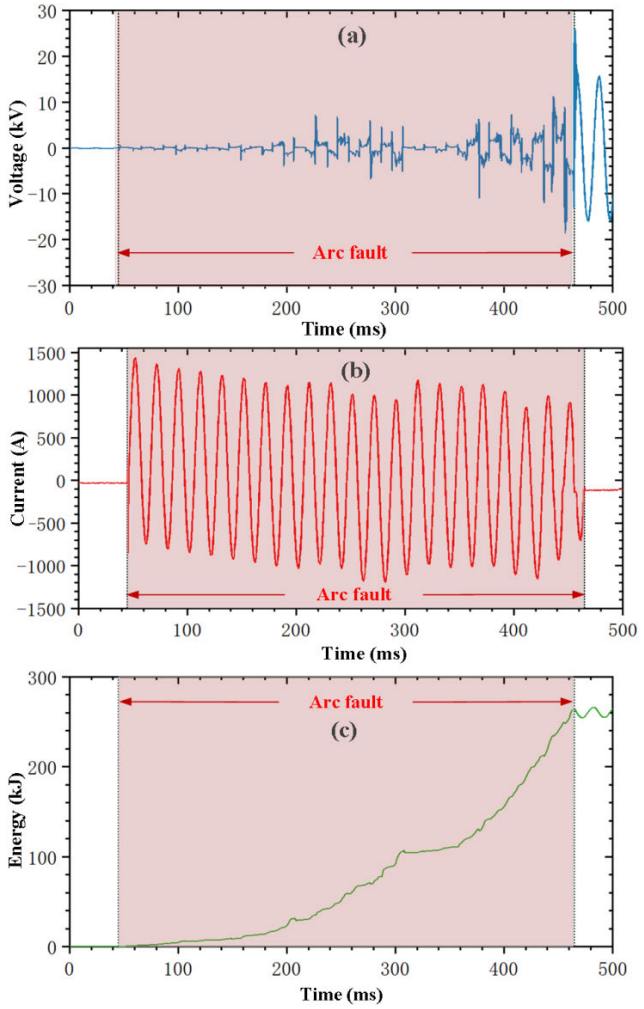

FIGURE 4. The arc voltage, current waveform, and energy in the 800 A arc fault test. (a) Voltage waveform. (b) Current waveform. (c) Energy waveform.

amplitude was low, fluctuating in the range of 0.3-0.5 kV, and gradually increased afterward, stabilizing at around 2 kV. After the arc was extinguished, the voltage immediately rose to 10 kV, the rated voltage of the power supply. The arc energy could be computed by real-time integration of the product of voltage and current. The total energy of the arc was calculated to be 264 kJ. Subsequent inspection of the critical junctures of the bushing and turret revealed no abnormalities after the test.

2) 1400A

During the 1400 A arc test, the test chamber experienced a rupture, turret detachment, oil and gas ejection, and combustion accompanied by a flash of fire. The rupture occurred at the transition flange, with bolts pulled out and threads damaged. Discharge marks were observed on the surface of the turret near the arc wire. The test results are illustrated in Fig. 5.

Arc voltage, current and energy measured in the 1400 A arc fault test are shown in Fig, 6.

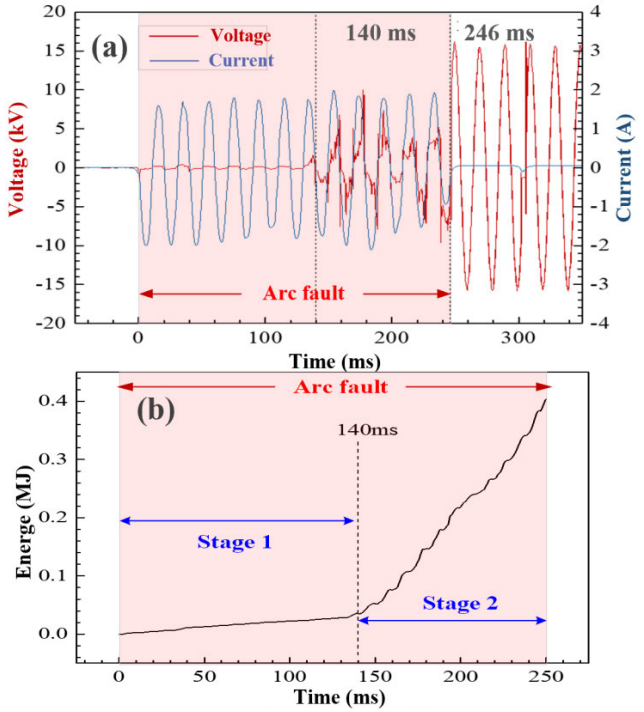

FIGURE 5. Turret explosion site in the 1400 A arc fault test.

FIGURE 6. Turret explosion site in the 1400 A arc fault test. (a) Voltage waveform and Current waveform. (b) Energy waveform.

As can be seen from Fig. 6, the arc burning time of this test was 246 ms, and the practical value of arc current was about 1400 A. The shortened arc time was attributed to the premature extinguishing of the arc caused by the rupture of the turret and the raised seat model. The results of arc voltage, current and energy measured in the arc fault test showed that the peak value of arc energy was about 400 kJ.

According to the arc voltage and current variation curves during turret rupture, the arc process can be divided into two stages, as shown in Fig. 6(b).

Stage 1: The peak value of arc voltage was relatively small, presenting a periodic waveform with a gradual change. The arc burning was relatively stable, characterized by a low rate of energy release within the time frame of 0-140 ms.

Stage 2: The arc voltage experienced a sudden increase in amplitude, with instantaneous peak values reaching up to 10 kV. It exhibited intense fluctuations superimposed on

the waveform, leading to a significant rise in the rate of energy release during the period of 140-246 ms. At 246 ms, the arc current was interrupted, and rupture and deflagrations occurred.

B. GAS PRODUCTION CHARACTERISTICS OF ARC FAULT INSULATING OIL

The gas generated in arc faults can be collected and analyzed by the gas-collecting device installed in the turret. Due to the explosion in the 1400 A arc test, a large amount of oil came into contact with the air, which may cause errors in the gas production results. Therefore, in this paper, only the oil samples after the 800 A arc test were analyzed by oil chromatography, and the gas samples collected through the air collection bag were analyzed by gas chromatography. The results of oil chromatography are shown in Fig. 7.

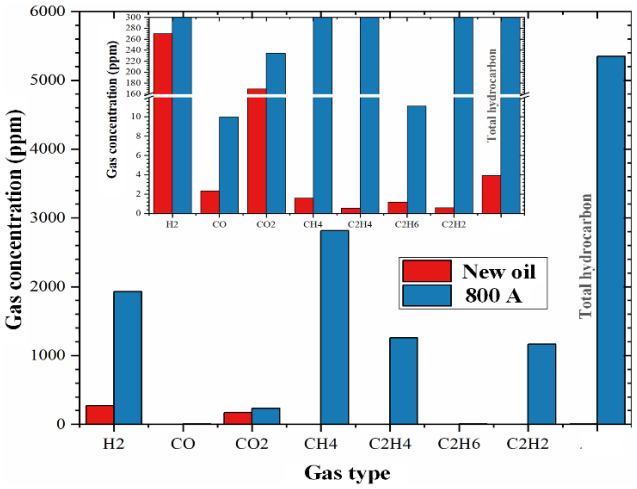

FIGURE 7. Oil chromatographic analysis after 800 A arc fault test.

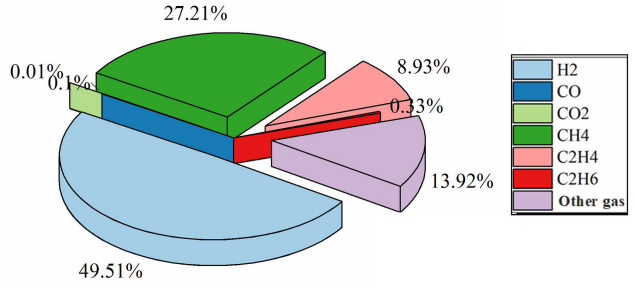

FIGURE 8. Gas chromatography analysis after 800 A arc fault test.

It is evident from the results that the content of various characteristic gases in the oil significantly increased following an arc fault, with gases such as C_2H_2, C_2H_4 showing an increase of more than 2000 times. The typical gases observed in the oil after discharge were mainly H_2, CH_4, C_2H_2 and C_2H_4, accounting for 1.51% of the total gas content. According to the three-ratio method, the calculated code value was 122, indicating the occurrence of an arc discharge and a high temperature of over 700 °C within the transformer. This observation was consistent with the experimental conditions.

The gas in the bag was analyzed through gas chromatography. As shown in Fig. 8, the spilled gas primarily consisted of H_2 and CH_4, which collectively accounted for more than 75% of the total gas volume, followed by a certain amount of C_2H_4, undetected macromolecular hydrocarbons and other gases. Since the tank was filled before the experiment, leaving no air inside, the content of O_2 and N_2 was below 1%, which was included in other gases here. In addition, trace amounts of CO, CO_2, and C_2H_6 gases were detected.

C. DEGRATION OF INSULATING OIL DUE TO ARC FAULT

During the test, the electrode and insulating oil material underwent carbonization, resulting in a large amount of black smoke that rapidly enveloped the arc. Consequently, the insulating oil became cloudy, as shown in Fig. 9. The presence of carbon particles in the oil will reduce the dielectric strength of the insulating oil and accelerate the deterioration of the oil [25], [26].

FIGURE 9. Turquoise insulation oil after 800 A arc fault.

The infrared spectrum analysis results of insulating oil after 800 A arc failure are shown in Fig. 10. Notable alterations were observed in the absorption peaks at 3000-2800 cm^{-1} and 1500-1200 cm^{-1}, indicating that high energy discharge resulted in significant changes in the position of the main absorption peaks of C-H. Consequently, the fundamental molecular structure of the primary elements, namely C and H, underwent changes. These changes were primarily manifested in the asymmetric stretching vibration and bending vibration peak associated with methyl and methylene C-H. The thermal stability of hydrocarbons determines the rate of decomposition of the oil, i.e., the rate of gas production; and the magnitude of the bond energy determines the thermal stability of the compound. Upon review, it is known that the bond energies of the C-H bond, C-C bond, C = C bond and C ≡ C bond increase in that order. When the insulating oil is cracked, alkanes are generated first, followed by olefins and finally alkynes. And when the oil temperature is close to 700 °C, it will also generate free carbon.

D. BREAKDOWN VOLTAGE ANALYSIS OF OIL SAMPLE AFTER ARC FAULTS

After two arc faults with peak currents of 800 A and 1400 A, 1 L of oil samples were individually taken for filtration

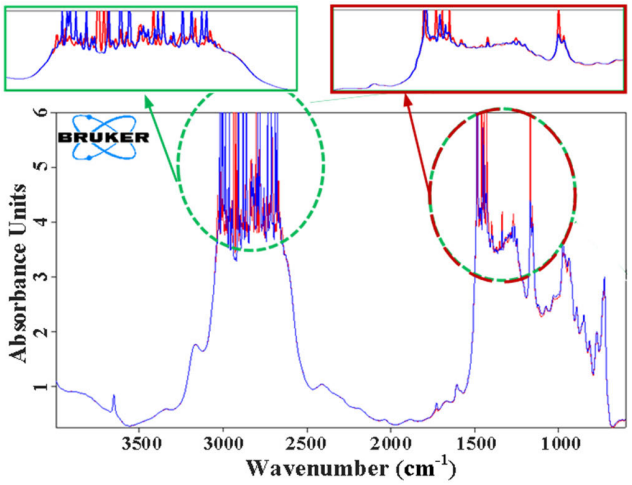

FIGURE 10. The infrared spectrum of insulating oil after the 800 A arc fault.

treatment. The untreated oil sample and the filtered counterpart were divided into four groups, and subjected to breakdown voltage testing according to the insulation oil breakdown voltage determination method specified in the national standard GB/T 507-2002.

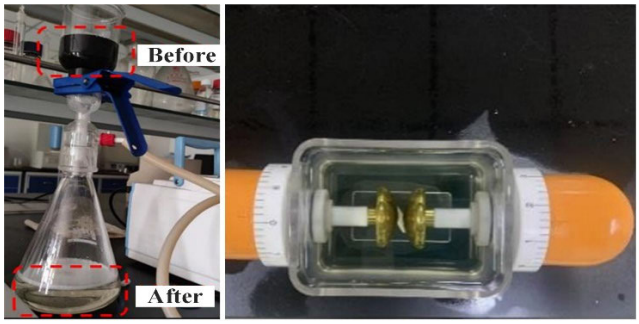

FIGURE 11. Oil sample processing and oil cup of breakdown voltage test.

The continuous voltage boost method was employed, wherein the sample was gradually pressurized at a rate of 2 kV/s between the electrodes until the breakdown occurred. The breakdown voltage was defined as the maximum voltage value when the circuit generated an arc. Once the breakdown voltage was reached, the corresponding value was recorded. Considering the impact of the electric field near the electrodes on the particle dispersion in the insulation oil during the pressurization process after each breakdown occurs, an electromagnetic mixer was used to stir the oil sample after each effective breakdown occurs. The power would be off for 2 minutes until the oil sample returned to a uniform state [27]. Subsequently, the pressurization process was repeated six times. The average value of 6 breakdown voltages was then calculated, and the results revealed that the breakdown voltage of transformer oil decreased by 33.75 kV (54.4%) after arc faults.

In a previous study [28], the Weibull statistical model was used for the fitting analysis of the breakdown voltages of four groups of oil samples, revealing that the breakdown voltages of the insulating oil follow a Weibull distribution. This paper used a two-parameter Weibull distribution model for statistical analysis of the test results. The expression of the two-parameter Weibull distribution model is shown as follows, where t represents the variable, α is the scale parameter, and β is the shape parameter.

$$F(t) = 1 - e^{-(t/\alpha)^{\beta}} \tag{1}$$

Based on the experimental data, a Weibull fitting was conducted, and the Weibull distribution test diagram and 63.2% breakdown voltage were obtained, as shown in Table 2 and Fig. 12.

TABLE 2. Results of breakdown voltage tests.

	800A	1400A
Average U_b after oil filtration / kV	62.00	28.25
63.2% U_b after oil filtration / kV	65.23	33.56
Average U_b of unfiltered oil / kV	29.00	21.60
63.2% U_b of unfiltered oil / kV	30.34	23.16

As shown in Fig. 12, the breakdown voltage data points of the four groups of samples are scattered on both sides of a straight line, confirming compliance with the presumed conditions of Weibull distribution. The sample of unfiltered oil exhibited a higher concentration of carbon particles, which migrated and accumulated in regions of high electric field intensity when subjected to the electric field force. The assembled carbon particles influenced the nearby electric field distribution, resulting in more significant distortion and even breakdown when they formed a small bridge of impurities. After the 1400 A current arc, the concentration of carbon particles in the insulating oil increased. As the concentration of carbon particles in the insulating oil rose, more carbon particles gathered in the high electric field area under the influence of the electric field, and these carbon particles subsequently aligned along the electric field lines to create small bridges of impurities. The rising carbon particle concentration facilitated the formation of these impurity bridges, which made them more likely to appear in the insulating oil. As a result, partial discharge was more likely to occur in the insulating oil, ultimately resulting in decreased breakdown voltage of the insulating oil. The normalized breakdown voltage values of the four groups of oil samples are shown in Fig. 13.

Similarly, the test results can be explained can also be explained by using Maxwell's solid-liquid mixture conductivity equation. The calculation equation for the conductivity of insulating oil containing carbon particles is shown below.

$$\gamma = \gamma_f \left[1 + \frac{3\varphi}{(\alpha+2)/(\alpha-1) - \varphi}\right] \tag{2}$$

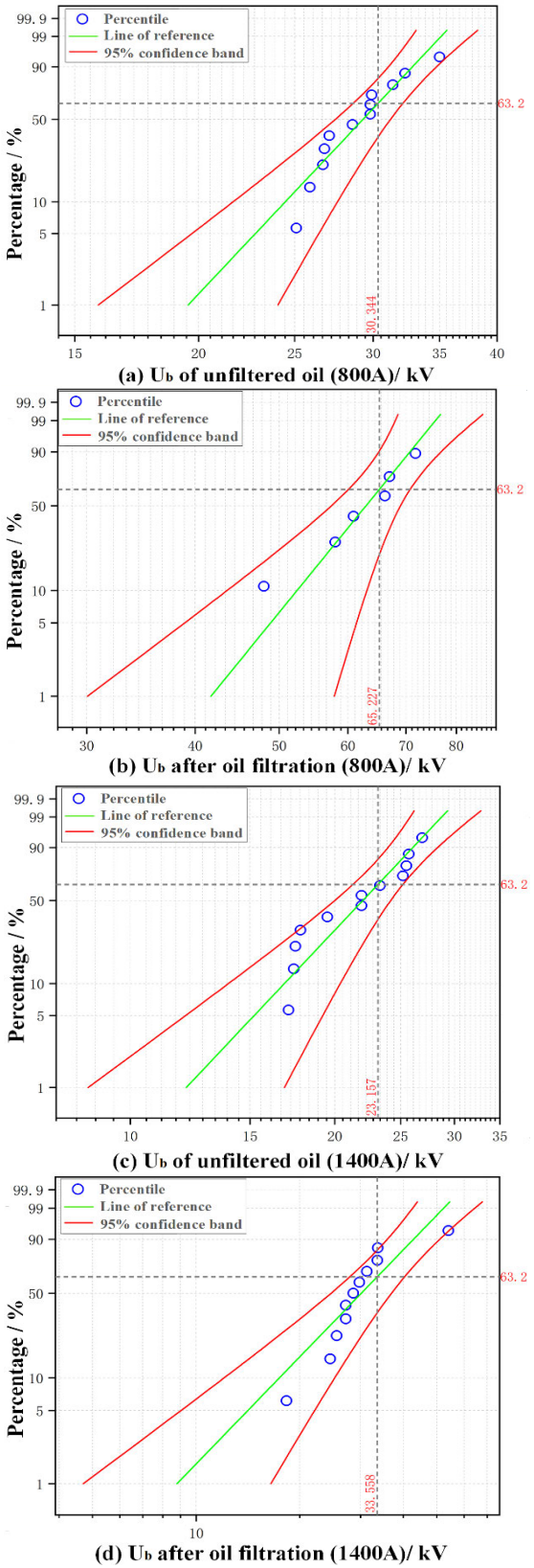

FIGURE 12. Weibull analysis on four groups of oil sample test data.

In the above equation, γ and γ_f represent respectively the conductivity of insulating oil containing carbon particles and non-carbon particles; $\alpha = \gamma_p/\gamma_f$ indicates the ratio of electrical conductivity of carbon particles to insulating oil, where γ_p is the electrical conductivity of carbon particles; φ is the volume percentage of carbon particles. The conductivity of carbon particles in the oil is much higher than that of insulating oil, so (2) can be simplified to (3).

$$\gamma = \gamma_f \left[1 + \frac{3\varphi}{1-\varphi}\right] \tag{3}$$

As the carbon particle in the insulation oil multiplied, a noticeable increase in the electrical conductivity of the oil sample was observed. As a result, the breakdown voltage of the oil sample decreased with an increasing concentration of carbon particles.

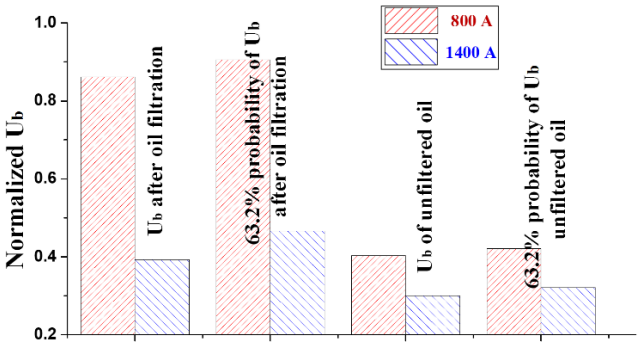

FIGURE 13. Normalized breakdown voltage values.

IV. QUANTITATIVE CHARACTERIZATION OF TURRET HIGH-ENERGY DISCHARGE

Based on the above analysis, it is evident that the energy generated by the discharge process is the most crucial cause of the thermal expansion of the turret and transformer component materials. The energy exerts significant pressure on the components, ultimately leading to their failure. Therefore, it is essential to monitor and quantify the energy discharged accurately. Fig. 14 shows a diagram of the energy flow of the high-energy discharge inside the transformer.

As shown in Fig. 14, the energy generated during the discharge process can be attributed to two primary sources: One is the Joule heat (Q_{arc}) generated directly by the discharge, and the other is the heat (Q_{oxd}) generated by the

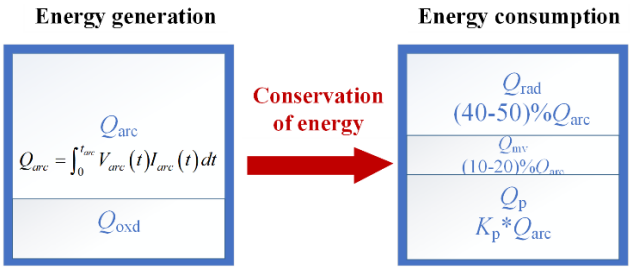

FIGURE 14. Schematic diagram of internal high-energy discharge energy flow.

chemical reaction of metal and other materials at the end of the bushing. However, the discharge energy was mainly converted into three kinds of energy, including radiant energy (Q_{rad}), metal melting and gasification energy (Q_{mv}), and gas-absorbed energy (Q_p).

A. ENERGY PRODUCTION

1) THE JOULE HEAT (Q_{ARC})

Q_{arc} is a function of arc current, voltage, and discharge time, as shown in (4).

$$Q_{arc} = \int_0^{t_{arc}} V_{arc}(t) I_{arc}(t)\, dt \tag{4}$$

In the above equation, V_{arc} is the arc voltage, I_{arc} is the arc current, and t_{arc} is the arc duration. For 50-60Hz currents, the general duration is 3 to 4 cycles. In most cases, the arc current can be quickly cut off by the relay protection device in the circuit.

When an arc fault occurs, the arc voltage and current are always in the same direction. No matter how the arc current direction changes, the arc always produces energy proportional to the duration.

Therefore, in the calculation process, V_{arc} can be generally regarded as a positive value, convenient for integral calculation in (4). I_{arc} takes the absolute value, and Q_{arc} is calculated as in (5).

$$Q_{arc} = \int_0^{t_{arc}} V_{arc}(t) \left|I_{arc}(t)\right| dt \tag{5}$$

In calculating AC arc energy, it is generally assumed that the current follows a sinusoidal waveform with a constant value. In this analysis, certain factors are considered negligible, such as the voltage drop near the cathode and anode, the voltage drop in the near pole region, and the spikes of arc and arc extinguishing. As such, the electric field intensity E per unit length of the arc column is a constant value in the half-wave cycle of each arc current [29]. These spikes occur only momentarily, typically around the current zero-crossing point. Hence, the contribution of the energy associated with these spikes to the overall arc energy is minimal, and ignoring it will not compromise the accuracy of the calculation. Thus, the arc voltage is only related to the arc length l at each instant, as shown in (6).

$$V_{arc} = El \tag{6}$$

Based on the above assumptions, the arc energy calculation formula is shown in (7).

$$Q_{arc} = \int_0^{t_{arc}} E \cdot l \cdot I_m \left|\sin(\omega t + \varphi)\right| dt \tag{7}$$

Since arc extinguishing typically occurs at the zero-crossing point of the current, the arc energy calculation is based on half of the current cycle as the calculation unit. The initial phase of the current is set at 0, and the discharge lasts for n current half cycles. Then,

$$Q_{arc} = \frac{2 \cdot n \cdot E \cdot l \cdot I_m}{\omega} \tag{8}$$

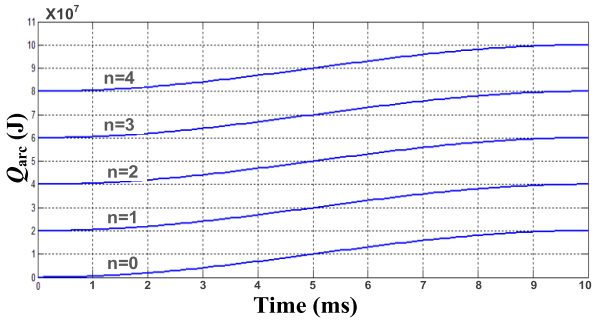

FIGURE 15. Arc energy curves.

According to the above test, the arc length is 10 cm, the arc current amplitude is 1000 A, and the frequency is 50 Hz. The energy change curve with time is shown in Fig. 15.

2) CHEMICAL REACTION HEAT (Q_{OXD})

The following reaction generally occurs during discharge for transformer bushings with copper end materials.

Studies have shown that when the discharge current is high, the heat Q_{oxd} generated by the oxidation reaction of copper is about 0.075 times the direct discharge energy Q_{arc}.

$$Cu + 1/2O_2 = CuO + 155kJ/mol \tag{9}$$

$$CuO + 1/2O_2 = Cu_2O + 168kJ/mol \tag{10}$$

B. ENERGY CONSUMPTION

The discharge energy was mainly converted into three kinds of energy, including radiant energy (Q_{rad}), metal melting and gasification energy (Q_{mv}), and gas-absorbed energy (Q_p). According to the law of conservation of energy, it can be seen that the total energy generated during the discharge process is equal to the sum of the energy flow, that is,

$$Q_{arc} + Q_{oxd} = Q_{rad} + Q_{mv} + Q_p \tag{11}$$

For the case of bushings with copper end materials, Q_{rad} during discharge accounts for about 40-50% of the directly generated heat Q_{arc}. The metal melting and gasification energy Q_{mv} accounts for about 10-20% of the Q_{arc}. By substituting these relationships into (6), the energy absorbed by the gas can be obtained.

$$Q_p \approx (30\% - 50\%)\, Q_{arc} + Q_{oxd} \tag{12}$$

In this paper, the energy absorbed by the gas is estimated as follows.

$$Q_p \approx 50\% Q_{arc} \tag{13}$$

Generally, the coefficient 50% is denoted as the factor denoted as K_p, which indicates the proportion of energy absorbed by the gas to the energy directly generated during the discharge. This proportion is a critical parameter that influences the calculation of gas shock pressure.

V. CONCLUSION

In this research, a test platform of arc discharge fault in the transformer turret was constructed, and the actual simulation test of arc discharge fault of 800 A and 1400 A was carried out. The energy conversion of the discharge arc within the turret and the insulating oil decomposition characteristics after arc faults were studied, and the following conclusions were obtained:

(1) The arc discharge fault in the transformer turret area was built and completed based on the specifications of the turret. That facilitated a true-simulation test of arc discharge fault with high current and deflagration capacity. The effective data of arc energy characteristic curve and corresponding voltage and current waveform were obtained.

(2) The test focused on exploring the high-energy discharge characteristics of the turret area under high current and high energy. Arc energy and arc current are important factors that affect the boost voltage in the turret. During the bushing rupture process under a high current (1400 A), the arc process can be divided into two stages. In the first stage, the peak value of arc voltage was relatively small, and the arc burning was relatively stable, characterized by a low energy release rate within 0-140 ms. In the second stage, the arc voltage experienced a sudden increase in amplitude, with instantaneous peak values reaching up to 10 kV, and the energy release rate increased significantly during the period of 140-246 ms. At 246 ms, the arc current was interrupted, and rupture and deflagrations occurred.

(3) After the arc fault, the content of various characteristic gases in the oil significantly increased, with gases such as C_2H_2, C_2H_4 showing an increase of more than 2000 times. The typical gases observed in the oil were H_2, CH_4, C_2H_2, and C_2H_4. The main gas produced by insulating oil decomposition caused by arc faults were H_2 and CH_4, which collectively accounted for more than 75% of the total gas volume.

(4) After the arc fault, the content of carbon particles in the insulating oil increased, which in turn resulted in the decreasing breakdown voltage of the oil sample. The breakdown voltage of the transformer oil dropped by 33.75 kV (54.4%).

(5) The energy during the discharge process is mainly derived from Q_{arc}. The discharge energy was mainly converted into Q_{rad}, Q_{mv}, and Q_p.

REFERENCES

[1] L. Zhenya, *UHV AC/DC Power Grid*, 2nd ed. Beijing, China: China Electric Power Press, 2013, pp. 1–5.

[2] L. Zhenya et al., "Findings in development of ±1100 kV UHV DC transmission," *Proc. CSEE*, vol. 40, no. 23, pp. 7782–7792, 2020.

[3] G. Chen, L. Peng, and H. Huiwen, "Research on 1100 kV and above UHV DC transmission technologies," *Proc. CSEE*, vol. 40, no. 20, pp. 6745–6754, 2020.

[4] H. Trencham, *Circuit Breaking*. London, U.K.: Butterworth, 1953, pp. 10–12.

[5] T. Tadokoro, M. Kotari, T. Ohtaka, and T. Amakawa, "Pressure fluctuation due to an underwater arc in a closed vessel containing air and water: Influence of depth of arc on pressure fluctuation," *IEEJ Trans. Power Energy*, vol. 134, no. 5, pp. 427–435, 2014.

[6] T. Tomo et al., "Pressure rises due to arc under insulating oil in closed vessel: Relationship between bubble behavior and pressure rises," *IEEJ Trans. Power Energy*, 2016.

[7] L. Mu, Y. Wang, W. Jiang, and F. Zhang, "Study on characteristics and detection method of DC arc fault for photovoltaic system," *Proc. CSEE*, vol. 36, no. 19, pp. 5236–5244, 2016.

[8] M. Binnendiljk, G. C. Schoonenberg, and A. J. W. Lammers, "The prevention and control of internal arcs in medium-voltage switchgear," in *Proc. 14th Int. Conf. Exhib. Electr. Distrib. (CIRED)*, Birmingham, U.K., 1997.

[9] J. Ruan, P. Li, and D. C. Huang, "Review on thermal-mechanical effects research of MV switchgear due to internal short circuit arcing," *High Voltage Eng.*, vol. 44, no. 10, pp. 3340–3351, 2018.

[10] W. R. Mahieu, "Prevention of high-fault rupture of pole-type distribution transformers," *IEEE Trans. Power App. Syst.*, vol. PAS-94, no. 5, pp. 1698–1707, Sep. 1975.

[11] A. Hamel, J. B. Dastous, and M. Foata, "Estimating overpressures in pole-type distribution transformers. Part I: Tank withstand evaluation," *IEEE Power Eng. Rev.*, vol. 22, no. 8, p. 70, Aug. 2002.

[12] J. B. Dastous, A. Hamel, and M. Foata, "Estimating overpressures in pole-type distribution transformers. Part II: Prediction tools," *IEEE Power Eng. Rev.*, vol. 22, no. 8, p. 70, Aug. 2002.

[13] R. Brady, S. Müller, G. L. de Bressy, P. Magnier, and G. Périgaud, "Prevention of transformer tank explosion: Part 2—Development and application of a numerical simulation tool," in *Proc. ASME Pressure Vessels Piping Conf.*, 2008, pp. 49–58.

[14] R. Brady, S. Müller, M. Petrovan-Boiarciuc, G. Perigaud, and B. Landis, "Prevention of transformer tank explosion: Part—Design of efficient protections using numerical simulations," in *Proc. ASME Pressure Vessels Piping Conf.*, Jul. 2009, pp. 667–675.

[15] M. Foata, M. Iordanescu, and C. Hardy, "Computational methods for the analysis of explosions in oil-insulated electrical equipment," *IEEE Trans. Power Syst.*, vol. 3, no. 1, pp. 286–293, Feb. 1988.

[16] C. Yan, Y. Xu, P. Zhang, S. Kang, X. Zhou, and S. Zhu, "Investigation of the gas bubble dynamics induced by an electric arc in insulation oil," *Plasma Sci. Technol.*, vol. 24, no. 4, Apr. 2022, Art. no. 044003.

[17] L. A. Darian, A. V. Kozlov, V. P. Polishchuk, M. N. Povareshkin, E. E. Son, V. E. Fortov, and A. V. Shurupov, "The arcless method of testing high-voltage oil-filled equipment for explosion safety," *Thermal Eng.*, vol. 58, no. 14, pp. 1196–1199, Dec. 2011.

[18] R. J. Ringlee and N. W. Roberts, "Tank pressures resulting from internal explosions," *Trans. Amer. Inst. Electr. Eng. III, Power App. Syst.*, vol. 78, no. 4, pp. 1705–1710, Dec. 1959.

[19] L. Zehong, L. Licheng, Z. Yuanxiang, Z. Zhiyi, H. Delin, and L. Yuhang, "Study on arc fault and pressure characteristics in transformer riser area," *Proc. CSEE*, vol. 41, no. 13, pp. 4688–4698, 2021.

[20] *Guide for Transformer Fire Safety Practices*, Cigre Brochure 537, Paris, France, 2013.

[21] N. Abi-Samra, J. Arteaga, B. Darovny, M. Foata, J. Herz, T. Lee, V. N. Nguyen, G. Perigaud, C. Swinderman, R. Thompson, G. Zhang, and P. D. Zhao, "Power transformer tank rupture and mitigation—A summary of current state of practice and knowledge by the task force of IEEE power transformer subcommittee," *IEEE Trans. Power Del.*, vol. 24, no. 4, pp. 1959–1967, Oct. 2009.

[22] *Fire Hazard Testing: Guidance for Assessing the Fire Hazard of Electro Technical Products—Insulating Liquids*, Standard IEC 60695-1-40.

[23] *Guide of Substation Fire Protection*, Standard IEEE 979.

[24] K. Goto and Y. Miura, "The pressure rise during the internal fault in oil-filled transformer," in *Proc. CIGRÉ SC12 Colloq.*, 1987.

[25] F. Atalar, A. Ersoy, and P. Rozga, "Experimental investigation of the effect of nano particles on the breakdown strength of transformer liquids by harmonic current analysis," *Electr. Power Syst. Res.*, vol. 221, Aug. 2023, Art. no. 109390.

[26] F. Atalar, A. Ersoy, and P. Rozga, "Investigation of effects of different high voltage types on dielectric strength of insulating liquids," *Energies*, vol. 15, no. 21, p. 8116, Oct. 2022.

[27] Q. Bo et al., "Interface charge characteristics of oil-paper insulation under non-uniform electric field," *Proc. CSEE*, vol. 33, no. 34, pp. 241–249, 2013.

[28] C. D. Lai and M. Xie, "Stochastic ageing and dependence for reliability," *Technometrics*, vol. 49, no. 2, p. 22, May 2007.

[29] S. Zhenqiu, "Drawing and application of AC arc energy calculation curve," *J. Xi'an Jiaotong Univ.*, pp. 81–95, 1963.

SHIHONG HU was born in China, in 1975. She is currently a Senior Engineer with State Grid Sichuan Electric Power Research Institute. Her research interests include transformer insulation oil and transformer fault diagnosis.

ZHICHENG HUANG was born in Henan, China, in 1993. He received the Ph.D. degree from North China Electric Power University, Beijing, China, in 2022. He is currently an Engineer with State Grid Sichuan Electric Power Research Institute. His research interests include insulation structure optimization design of power equipment, multi-physics field simulation, and electrical contact characteristics.

XI LIU was born in China, in 1982. She received the M.Sc. degree in high voltage and insulation technology from Southwest Jiaotong University, in 2007. Her research interest includes the insulation monitoring of power transformers.

JIAHUI CHEN was born in China, in 1991. She received the Ph.D. degree from Tsinghua University, in 2018. She is currently a Senior Engineer with State Grid Sichuan Electric Power Research Institute. Her research interests include metal materials, processes, and devices for power grid equipment.

YAN WANG was born in Shangqiu, Henan, China, in 1993. She received the Ph.D. degree in organic chemistry from Sichuan University, Chengdu, China. Her research interests include insulation oil analysis and transformer fault diagnosis.

TAO ZHAO (Member, IEEE) was born in Baoding, Hebei, China, in 1982. He received the B.Eng. degree from North China Electric Power University, in 2005, the M.Sc. degree from Chongqing University, in 2008, and the Ph.D. degree from North China Electric Power University, in 2017. His research interests include the insulation monitoring of power transformers and fault detection and diagnosis of electric equipment.

CHAOJIE YANG was born in China, in 1993. He is currently pursuing the Ph.D. degree in electrical engineering with North China Electric Power University, Baoding, China. His research interest includes the insulation monitoring of power transformers.